



41 Using weather generators, long simulations of weather variables provide accurate descriptions of the
42 climate system and can be used for natural hazard assessments. Among the large panel of existing
43 weather generators, stochastic ones are used to construct, via a stochastic generation process, single
44 or multisite time series of predictands (e.g. precipitation, temperature) based on the distributional
45 properties of observed data. These characteristics, and consequently the weather generator
46 parametrisation, are usually determined on a monthly or seasonal basis to take seasonality into
47 account. They can also be estimated for different families of atmospheric circulation, often referred
48 to as weather types. A state of the art of the most common methods which have been used for the
49 downscaling of precipitation (single or multi-site) is presented in Wilks (2012) or in Maraun et al.,
50 (2010). More recent publications gather detailed reviews of some sub-categories of weather
51 generators (e.g. Ailliot et al., 2015 for hierarchical models). An increasing number of studies focuses
52 on the generation of multivariate and/or multi-site series of predictands (e.g. Steinschneider and
53 Brown, 2013; Srivastav and Simonovic, 2015; Evin et al. 2018a; Evin et al. 2018b). Stochastic weather
54 generators are able to produce large ensembles of weather time series presenting a wide diversity of
55 multiscale weather events. For all these reasons, they have been used for a long time to enlighten
56 the sensitivity and possible vulnerabilities of socio-eco-systems to the climate variability (Orlowsky et
57 al. 2010) and to weather extremes.

58

59 Another family of models used for the generation of weather sequences is the analogue method.
60 Since the description of the concept of analogy by Lorenz (1969), the analogue method has gained
61 popularity over time for climate or weather downscaling. This analogue model strategy has been
62 applied in many studies (Boe et al., 2007; Abatzoglou and Brown, 2012; Steinschneider and Brown
63 2013) and has been used to address a wide range of questions from past hydroclimatic variability
64 (e.g. Kuentz et al, 2015; Caillouet et al., 2016) to future hydrometeorological scenarios (e.g. Lafaysse
65 et al., 2014; Dayon et al., 2015). The standard analogue approach hypothesises that local weather
66 parameters are steered by synoptic meteorology. A set of relevant large scale predictors is used to
67 describe synoptic weather conditions. From the atmospheric state vector, characterizing the synoptic
68 weather of the target simulation day, atmospheric analogues of the current simulation day are
69 identified in the available climate archive. Then, the analogue method makes the assumption that
70 similar large scale conditions have the same effect on local weather. The local or regional weather
71 configuration of one of the analogue days is then used as a weather scenario for the current
72 simulation day. The key element of the analogue method is that it does not require any assumption
73 on the probability distributions of predictands. This is a noteworthy advantage for predictands, such
74 as precipitation, which have a non-normal distribution with a mass in zero. Most of the studies using
75 analogues focused on precipitation and temperature either for meteorological analysis (Chardon,
76 2014; Daoud, 2016), or as inputs for hydrological simulations (Marty, 2012; Surmaini et al., 2015).
77 Nevertheless, analogues are increasingly used for other local variables such as wind, humidity
78 (Casanueva et al., 2014) or even more complex indices (e.g. for wild fire, Abatzoglou and Brown,
79 2012). When multiple variables are to be downscaled simultaneously, another major advantage of
80 the analogue method is that the different predictands scenarios are physically consistent and the
81 simulated weather variables are bound to reproduce the correlations between the variables (e.g.
82 Raynaud et al., 2017) and sites (Chardon et al., 2014). Indeed, when analogue models use the same
83 set of predictors (atmospheric variables and analogy domains) for all predictands, all surface weather
84 variables and sites are sampled simultaneously from the historical records, thus preserving inter-site
85 and inter-variable dependency.

86

87 The two simulation approaches (stochastic weather generators and analog methods) described
88 above present some important advantages for the generation of long weather series but also some
89 sizeable drawbacks. Indeed, stochastic weather generators rely on strong assumptions on the
90 statistical distributions of predictands. Identifying the relevant mathematical representations of the
91 processes and achieving a robust estimation of their parameters can be difficult, especially if the
92 length of the meteorological records is short. Modelling the spatial-temporal dependency between



93 variables/sites is an additional challenge. Conversely, for the analogue-based approaches, the
94 identification of relevant atmospheric variables providing good prediction skills is not
95 straightforward. The limited length of local weather records is also a critical issue since resampling
96 past observations restricts the range of predicted values. In particular, the simulation of unobserved
97 values of predictands is not possible. This can be problematic if one is interested in estimating
98 possible extreme values of the considered variable. Furthermore, the information on synoptic
99 atmospheric conditions required by analog methods are generally coming from atmospheric
100 reanalyses, which also have a limited temporal coverage (e.g. from the beginning of the 20th century
101 for ERA20C, Poli et al., 2013) and from the mid-19th century for 20cr (Compo et al. 2011). The length
102 of the generated time series is thus typically bounded by the length of the reanalyses.

103
104 In this study we propose a weather generator (hereafter SCAMP+) building upon the SCAMP
105 approach presented by Chardon et al. (2018) and making use of reshuffled atmospheric trajectories,
106 following some of the developments by Buishand and Brandsma (2001) and Yiou et al. (2014). The
107 weather scenarios generated by SCAMP being limited by the coverage of the climate reanalyses, the
108 SCAMP+ model extends the pool of possible atmospheric trajectories. Using random transitions
109 between past atmospheric sequences, SCAMP+ generates unobserved atmospheric trajectories, on
110 which the 2-stage SCAMP approach can be applied. By exploring a wide variety of atmospheric
111 trajectories, SCAMP+ introduces some additional large-scale variability which improves the
112 exploration of possible weather sequences. In addition, as done in SCAMP (Chardon et al., 2018), the
113 SCAMP+ approach includes a simple stochastic weather generator which is estimated, for each
114 generation day, from the nearest atmospheric analogs of this day. These two steps (random
115 atmospheric trajectories and random daily precipitation/temperature values) improve the
116 reproduction of extreme values, overcoming previous limitations of analog-based weather
117 generators, usually known to underestimate observed precipitation extremes.

118
119 These developments are carried out for the exploration of hydrological extremes (extreme floods) of
120 the Aare River basin in Switzerland (Andres et al. 2019a,b). Meteorological forcings, i.e. temperature
121 and precipitation, are thus simulated to be used as inputs of a hydrological model, for different sub-
122 basins of the Aare river basin. Meteorological simulations from SCAMP+ have been used in the Swiss
123 EXAR project¹ and have proven its ability to estimate the discharge values associated to very large
124 return periods on the Aare River. In section 2, we describe in details the test region, the data and
125 three simulation approaches (a classical analogue method, referred to as ANALOGUE, SCAMP and
126 SCAMP+). Section 3 presents the main results on both climatological characteristics and extreme
127 values. Section 4 sums up the main outputs of this study and proposes some further developments
128 and analysis.

129
130

131 **3. Data and Method**

132 **3.1 Studied region**

133 This study is carried out on the Aare River basin which covers almost half of Switzerland (17,700
134 km²). The topography varies greatly within the basin with, on one hand, high mountains on its
135 southern part (maximum altitude of 4270 m, Finsteraarhorn) and on the other hand, plains on the
136 northern part (minimum altitude of 310 m). These different characteristics coupled with the basin
137 being located at the crossroads of several climatic European influences give a wide diversity of
138 possible weather situations across the year.

¹ <https://www.wsl.ch/en/projects/exar.html>



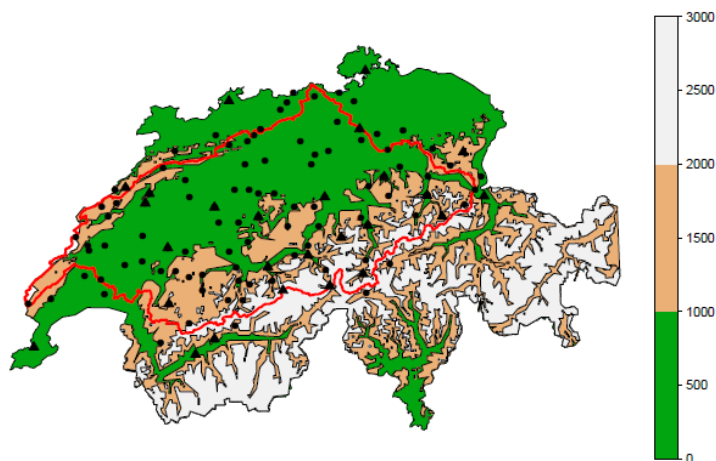
139

140 3.2 Atmospheric reanalysis and local weather data

141 The application of the analogue method requires a long archive providing an accurate description of
142 both past synoptic weather patterns and local atmospheric conditions. Indeed, a wide panel of
143 meteorological situations available for resampling is necessary in order to identify the best analogs
144 for the simulation (e.g. Van Den Dool et al., 1994 ; Horton et al., 2017). In most studies, synoptic
145 situations are provided by atmospheric reanalyses. Here, we use the ERA-20C atmospheric reanalysis
146 (Poli et al., 2013) which provide information on large scale atmospheric patterns on a 6 h basis from
147 1900 to 2010. Data are available at a 1.25° spatial resolution. More specifically, the set of predictors
148 used for the identification of atmospheric analogues is made of the geopotential height at 500 and
149 1000 hPa, the vertical velocities at 600 hPa, large scale precipitation and temperature. The
150 justification of these choices will be given in section 3.3.1.

151 The local and surface weather parameters of interest are retrieved from 105 weather stations for
152 precipitation and 26 weather stations for temperature, which are spread out homogeneously over
153 our target region, as presented on Figure 1. These data are available at a daily time step from 1930 to
154 2014. They have been spatially aggregated in order to obtain daily time series of mean areal
155 precipitation (MAP) and temperature (MAT) for the Aare region. The three weather generators
156 considered in this study aims at producing scenarios of daily time series of MAP and MAT. It can be
157 noticed that many applications of analogue-based approaches produce simulations at specific
158 weather stations. However, as shown by Chardon et al. (2016) for France, the prediction skill is
159 significantly improved when the prediction is produced for areal averages, which motivates the
160 generation of MAP and MAT values in this study.

161



162

163 **Fig.1: The Aare River basin (red) and locations of the different precipitation (dots) and temperature**
164 **(triangles) stations.**

165



166 3.3 Description of the three models

167 This section presents the three different models considered and evaluated in this study.

168

169 3.3.1 **ANALOGUE**: Classical analogue model

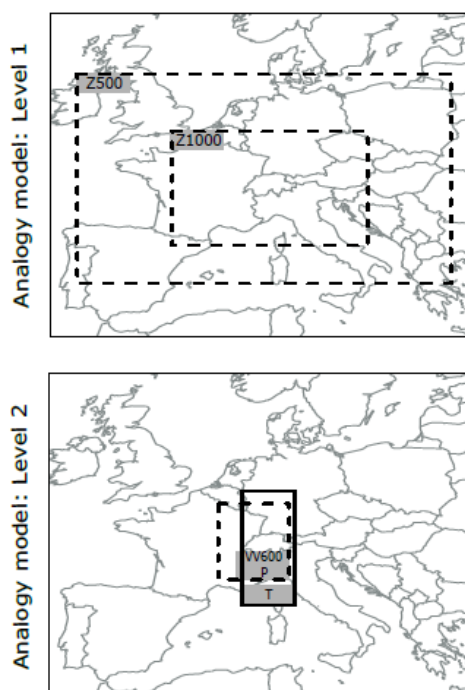
170 The most basic model evaluated in this study, hereafter referred to as ANALOGUE, relies on a
171 standard 2-level analogue method. For each day of the simulation period, a first set of analogue
172 dates is selected based on the predictors described in Raynaud et al. (2017) which guarantees both
173 inter-variable physical consistency and good predictive skills for 4 predictands (precipitation,
174 temperature, solar radiation and wind). In the present work, the predictors are defined as follows:

175 - The first level of analogy is based on daily geopotential heights at 1000 hPa and 500 hPa (HGT1000,
176 HGT500) as proposed by Horton et al. (2012) and Raynaud et al. (2017). From September to May, the
177 analogy is based on the geopotential fields on both the current day D and its following day D+1 at
178 12UTC. Thereby, the motions of low-pressure systems and fronts are better described and the
179 prediction skill of the method for precipitation is improved (e.g. Obled et al. 2002; Horton and
180 Brönnimann, 2019). In summer, only the geopotential fields on the current day are used as no similar
181 improvement could be found with a two-day analogy. 100 analogues are selected for each day of the
182 target period.

183 - The predictors selected for the second level of analogy derive from the best predictors sets
184 identified in Raynaud et al. (2017). From September to May, they are the vertical velocities at 600
185 hPa and the large scale temperature at 2 meters. In summer, the vertical velocities but also other
186 predictors such as the Convective Available Potential Energy (CAPE) led to a rather poor prediction of
187 precipitation due to the coarse resolution of the atmospheric reanalysis, which prevent it from
188 providing an accurate simulation of convective processes. Consequently, large scale precipitation
189 from the reanalysis has been used instead, resulting in predictive skills similar to the ones obtained
190 for the rest of the year. This second analogy makes a sub-selection of 30 analogues within the 100
191 analogues identified in the first analogy level.

192 The dimensions and position of the different analogy windows used to compute the analogy
193 measures are presented on Figure 2. They follow the recommendations for the analogy windows
194 optimisation presented in Raynaud et al. (2017) for all predictors.

195 With this 2-step analogy, 30 scenarios of daily MAP and daily MAT are generated for each day of the
196 simulation period (1900-2010). Combined with the Schaake Shuffle method described in section
197 3.3.4, the application of the ANALOGUE model leads to 30 scenarios of 110-year time series of daily
198 MAP and MAT.



199

200 **Fig.2: Positions and dimensions of the analogy windows in the analogue model at both analogy levels. Z500,**
 201 **geopotential at 500 hPa ; Z1000, geopotential at 1000 hPa ; VV600, vertical velocities at 600 hPa ; P,**
 202 **precipitation ; T, temperature.**

203

204 **3.3.2 SCAMP: Combined analog / generation of MAP and MAT values**

205 The SCAMP model enhances the previous approach ANALOGUE which is not able to generate daily
 206 values exceeding the range of observed precipitation and temperature. SCAMP combines the
 207 analogue method with a day-to-day adaptive and tailored downscaling method using daily
 208 distributions adjustment (Chardon et al. 2018).

209 For each prediction day, the following discrete-continuous probability distribution proposed by Stern
 210 and Coe (1984) is fitted to the 30 MAP values obtained from the atmospheric analogues of this day:

211
$$F_Y(y) = (1 - \pi) + \pi \cdot F_{GA}(y|y > 0, \alpha, \beta), \quad (1)$$

212 where π is the precipitation occurrence probability, F_{GA} is the gamma distribution parameterized
 213 with a shape parameter $\alpha > 0$ and a rate parameter $\beta > 0$. The π parameter is directly estimated by
 214 the proportion of dry days, and the parameters α, β of the gamma distribution are estimated by
 215 applying the maximum likelihood method to the positive precipitation intensities among the 30 MAP
 216 values. 30 MAP values are then sampled from the distribution model (1) in order to obtain
 217 unobserved values of precipitation, possibly beyond past observations. When there are less than 5
 218 positive MAP intensities in the analogues, we simply retrieve the MAP analog values. This distribution



219 model corresponds to a simplified version of the combined analog/regression model described in
220 Chardon et al. 2018 and we refer the reader to this paper for further information.

221 Similarly, for each prediction day, a Gaussian distribution $F_N(\mu, \sigma)$ is fitted to the 30 MAT values
222 obtained from the analogues. A sample of 30 new MAT values is then generated from this fitted
223 Gaussian distribution.

224 As for the ANALOGUE approach, the Schaake Shuffle reordering method is applied to the daily
225 scenarios obtained from SCAMP. 30 scenarios of 110-year time series of daily MAP and MAT are
226 produced.

227

228 3.3.3 SCAMP+

229 As mentioned previously, the first limitation of the analogue method is related to the length of the
230 synoptic weather information that is used to generate local predictands time series. In the present
231 case, the length of time series that can be produced with the models ANALOGUE and SCAMP is
232 limited to 110-year long weather scenarios.

233

234 In SCAMP+, we extend the archive of synoptic weather information by rearranging the synoptic
235 weather sequences, thus creating new atmospheric trajectories, used in turn as inputs to SCAMP.
236 This generation of new trajectories makes use of atmospheric analogues, following those of the
237 principles proposed in the weather generators described by Buishand and Brandsma (2001) and Yiou
238 et al. (2014). For any given day, the atmospheric synoptic weather is considered to have the
239 possibility to change its trajectory. The main hypothesis of this generation module is that if two days
240 J and K are close atmospheric analogues with atmospheric patterns heading in the same direction,
241 then their “future” are exchangeable and one could jump from one atmospheric trajectory to the
242 other. In other words, day $J+1$ is a possible future of day K and conversely day $K+1$ is a possible future
243 of day J . The probability p to jump from one trajectory to any other is considered as a parameter to
244 estimate.

245

246 The principle of a random atmospheric trajectory generation is sketched on Figure 3. In the present
247 work, the only predictor involved to compare the synoptic atmospheric configuration between 2
248 different days is the geopotential height field at 1000 hPa, for both the present day and its followers.
249 The spatial analogy domain is the one used in Philipp et al. (2010) for the identification of Swiss
250 weather types. The first line of Figure 3 presents an observed atmospheric trajectory in HGT1000
251 from February 8th to February 12th 1934. On the February 9th, we look for analogues of the current
252 day and its following day $D+1$. This is done to ensure that the two initial states are similar (high
253 pressure system located over France on February 9th 1934 and on its analogue, January 28th 1921)
254 and that the main features move in similar directions (high pressure system heading South-East on
255 both February 10th 1934 and January 29th 1921).

256

257 Practically, the five best analogues of the current atmospheric 2-day sequence are identified and one
258 of those sequences is then selected with a probability p to generate the new day of the new
259 trajectory. The same method is repeated for this new day to find its future day (as illustrated in
260 Figure 3 for the sequence January 30th 1921 - February 12th 1925) and extend the new trajectory with

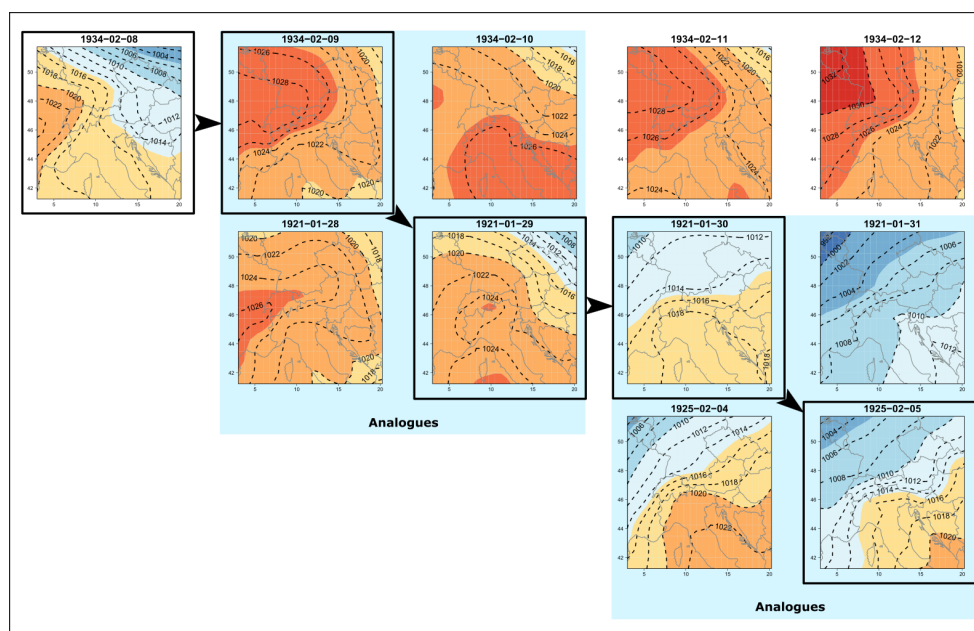


261 one additional day. This process is repeated as long as necessary. In the present work, it was used to
262 generate a 1000-year trajectory of daily synoptic weather situations. Rather large differences
263 between the synoptic weather situation can be obtained after some days between the observed
264 atmospheric sequence (e.g. February 12th 1934) and the random atmospheric trajectory (February
265 12th 1925). As we will show later on, such a method leads to higher weather variability at multiple
266 time scales.

267

268 To insure that two consecutive days of the generated sequences belong to the appropriate season,
269 the five 2-day analogue sequences are identified within a +/-15-day moving window centred on the
270 calendar day of the target simulation day (e.g. all June days if the target day is xxxx-06-15th).

271

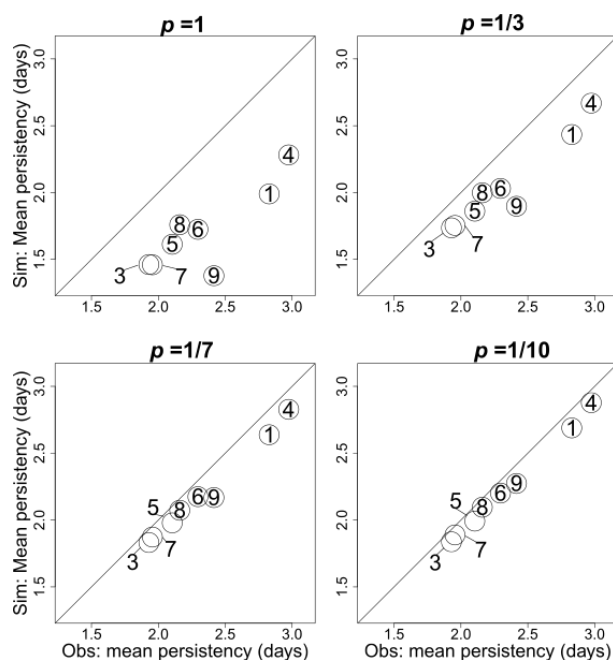


272

273 **Fig.3: Construction of a new 5-day atmospheric trajectory from an observed synoptic weather sequence.**
274 **Each sub-figure presents the geopotential at 1000hPa on the domain of interest. The black squares and**
275 **arrows give the new atmospheric trajectory and the blue shading highlights the two-day analogue that helps**
276 **“changing of atmospheric direction”.**

277

278 The transition probability p from one observed trajectory to another indirectly determines the level
279 of persistency of synoptic configurations. In this study, it has been calibrated in order to guarantee a
280 good climatology of the large scale atmospheric sequences. To do so, we analysed the mean
281 frequency and duration of each of the 9 weather types proposed for Switzerland by Philipp et al.
282 (2010) in the observed synoptic series and in different reconstructed ones for transition probability p
283 ranging from 1/10 (one transition every 10 days in average) to 1 (one transition per day in average).
284 The results presented on Figure 4 shows that a transition probability of 1/7 is necessary to generate
285 atmospheric trajectories that present a relevant persistency within each weather type.



286

287 **Fig.4: Mean persistence of each of the 9 weather types (indicated by the different circles in each panel), as**
288 **defined by Philipp et al. (2010), in the observed time series and in the simulated ones for transition**
289 **probabilities ranging from 1 to 1/10 for the generation of atmospheric trajectories.**

290

291 The long time series of synoptic weather generated with the above approach is further used as
292 inputs to the SCAMP generator described in the previous section. The SCAMP+ approach leads to 30
293 scenarios of daily MAP and MAT, each of these scenarios being based on the 1000-year random
294 atmospheric trajectories sequence. The output of this approach, combined with the Schaake Shuffle
295 method described in the next section, is thus composed of 30 scenarios of 1000-year time series of
296 daily MAP and MAT.

297

298 3.3.4 Temporal consistency: Application of the Schaake Shuffle

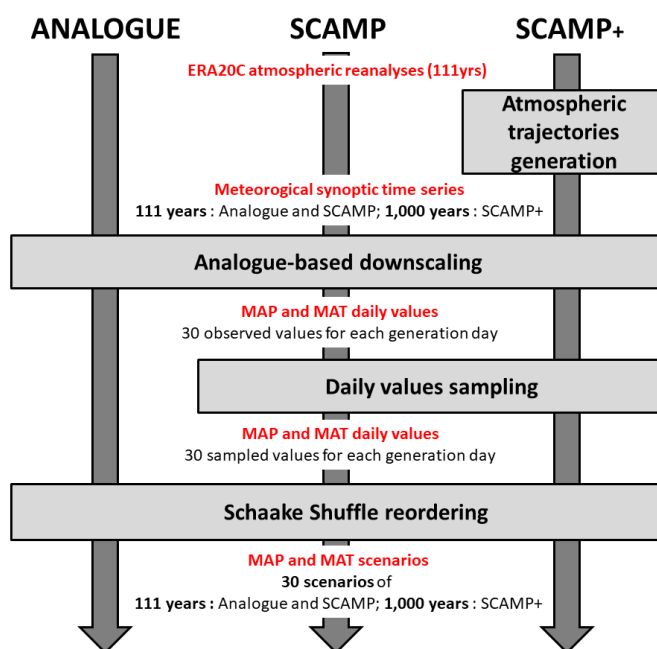
299 For each model (ANALOGUE, SCAMP and SCAMP+), 30 scenarios of daily MAP and MAT are
300 produced. To improve the temporal/physical consistency between two consecutive days or between
301 the temperature and precipitation scenarios (partially induced by the synoptic weather series), we
302 use the Schaake Shuffle method initially proposed by Clark et al. (2004). This method makes use of
303 both the inter-variable physical and the intra-variable temporal consistency in observations to
304 combine, at best, the outputs of any weather generator and reconstruct consistent predictands time
305 series. It is particularly useful if one is interested in generating relevant precipitation accumulation
306 scenarios over several days. A full description of the Schaake Shuffle method can be found in Clark et
307 al. (2004) and some applications can be found in Bellier et al. (2017) or in Schefzik (2017). Here, the
308 Schaake Shuffle consists in modifying the sequences of MAP and MAT values, preserving the



309 association of the ranks of MAP and MAT and rearranging sequences between days D and D+1.
310 Shuffled MAP and MAT sequences between consecutive days then have similar associations than
311 what has been observed. In this study, we give priority to the temporal consistency of precipitation
312 first. Temperature scenarios are recombined in a second step.

313 The different components of the models ANALOGUE, SCAMP and SCAMP+ are summarized in Figure
314 5.

315



316

317 **Fig.5: Illustration of the different steps applied (grey boxes) with models ANALOGUE, SCAMP and SCAMP+.**
318 **Outputs obtained after each step are indicated in red.**

319

320 4. Results

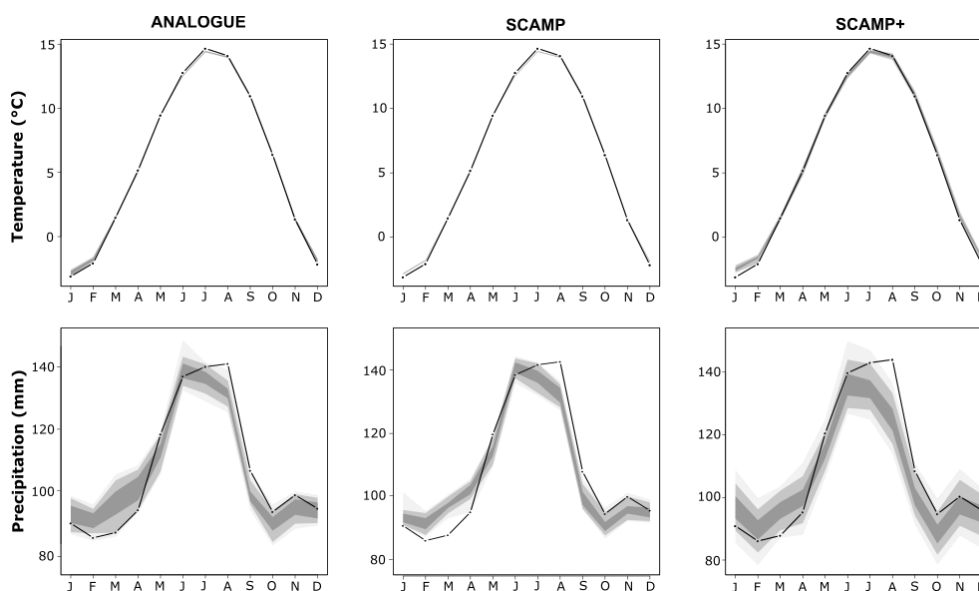
321 This section presents different statistical properties of the scenarios obtained with the 3 models and
322 discusses the performances of each model by comparison with observed statistical properties. For
323 the sake of consistency between the outputs, we compare the 30 scenarios of 111 years obtained
324 from ANALOGUE and SCAMP to 300 scenarios of 100 years from SCAMP+ (i.e. each scenario of 1,000
325 years is divided into 10 scenarios of 100 years).

326 4.1 Climatology

327 For both temperature and precipitation, the 3 models lead to an accurate simulation of their
328 seasonal fluctuations (Figure 6). However, one can notice the slight overestimation of winter



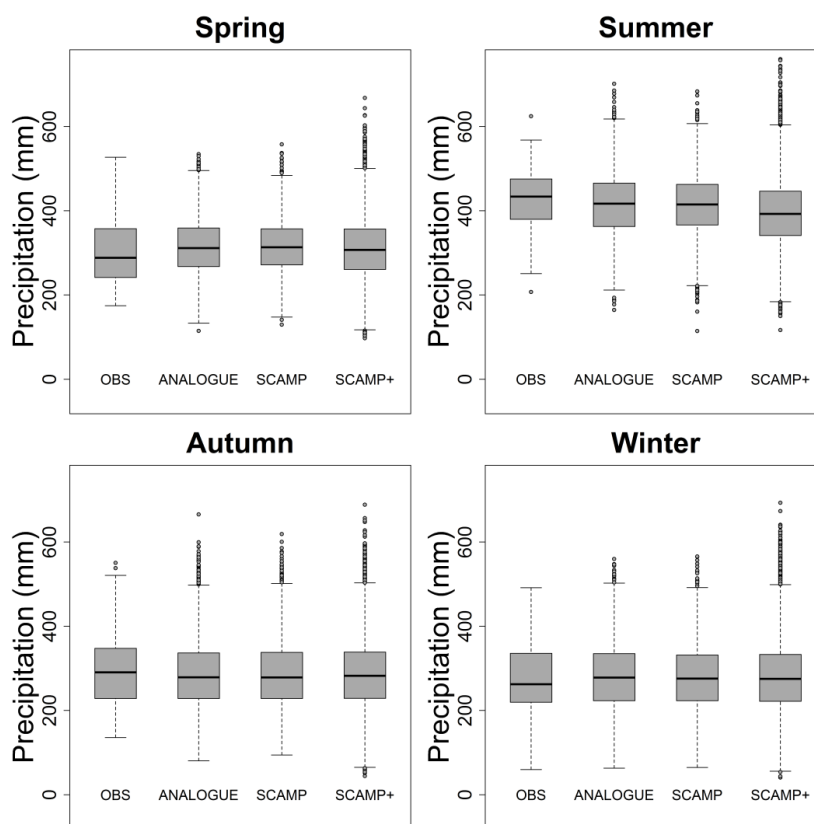
329 temperature and an underestimation of July and August precipitation. SCAMP also tends to have a
330 smaller inter-annual variability compared to ANALOGUE and SCAMP+.



331

332 **Fig.6: Observed and simulated seasonal cycles of temperature and precipitation for ANALOGUE, SCAMP and**
333 **SCAMP+. The grey shadings present the inter-quantiles intervals. Simulated seasonal cycles are obtained**
334 **using 30 scenarios of 111 years from ANALOGUE and SCAMP and 300 scenarios of 100 years from SCAMP+.**

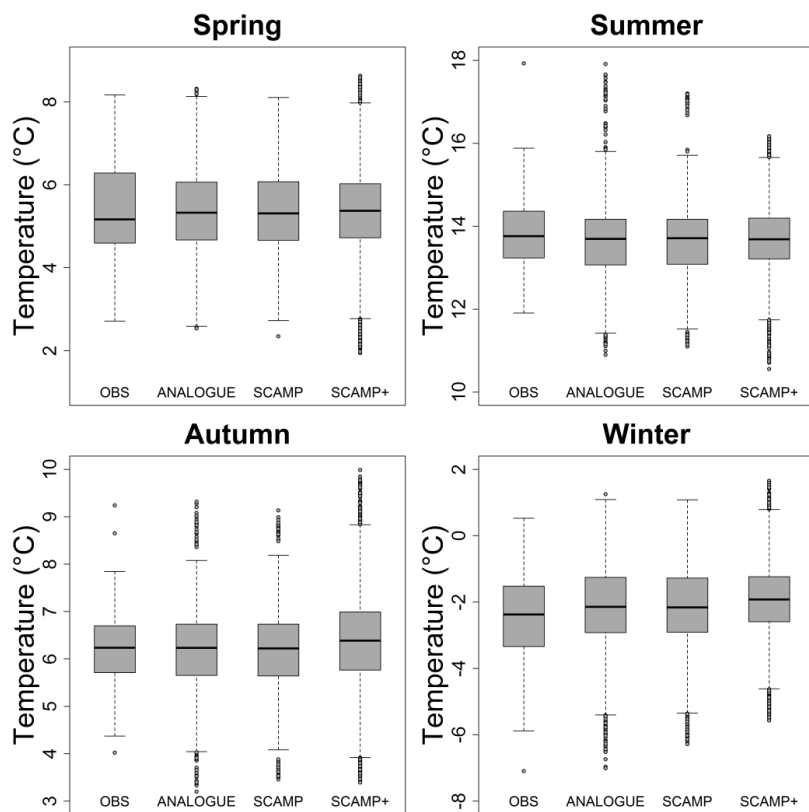
335 The distributions of seasonal precipitation amounts and seasonal temperature averages are
336 presented in Figure 7. Whatever the season, the three models are able to generate drier and wetter
337 seasons than the observed ones (Figure 7a). The very similar results obtained for ANALOGUE and
338 SCAMP suggest that the daily distribution adjustments used in SCAMP do not introduce more
339 variability at the seasonal scale. SCAMP+ is able to generate seasonal values that significantly exceed
340 the maximum values simulated by ANALOGUE and SCAMP (by 100 mm to 200 mm). This strongly
341 suggests that a large part of the seasonal variability comes from the variability of the synoptic
342 weather trajectories, the unobserved weather trajectories produced by SCAMP+ leading to a wider
343 exploration of extreme seasonal values.



344

345 **Fig.7a: Observed and simulated boxplots of seasonal precipitation amounts for ANALOGUE, SCAMP and**
346 **SCAMP+ (Spring: March, April, May. Summer: June, July, August. Autumn: September, October, November.**
347 **Winter: December, January, February).**

348 The same comments can be made for spring and autumn temperatures (Figure 7b). For those
349 variables however, SCAMP+ fails to simulate extremely hot summers or cold winters. This result is
350 probably due to the non-stationary climate conditions experienced during the 20th century. Creating
351 new atmospheric trajectories mixes synoptic sequences from the first half of the century with others
352 from the early 2000s. The much coolest conditions prevailing until the 1980s result in few chances to
353 generate seasonal temperature hotter than the 2003 summer for instance. This limitation will be
354 further discussed in the next section.



355

356 **Fig.7b: Observed and simulated boxplots of mean seasonal temperature for models ANALOGUE, SCAMP and**
357 **SCAMP+ (Spring: March, April, May. Summer: June, July, August. Autumn: September, October, November.**
358 **Winter: December, January, February).**

359

360 4.2 Daily Precipitations Extremes

361

362 As mentioned in section 1, simple analogue methods cannot simulate unobserved precipitation
363 extremes at the temporal resolution of the simulation (here daily). Moreover, for higher aggregation
364 durations, they also tend to underestimate observed precipitation extremes. Figure 8 presents the
365 precipitation values obtained with the three models for different return periods (from 2 year to 200
366 years) and different aggregation durations (from 1 to 5 days).

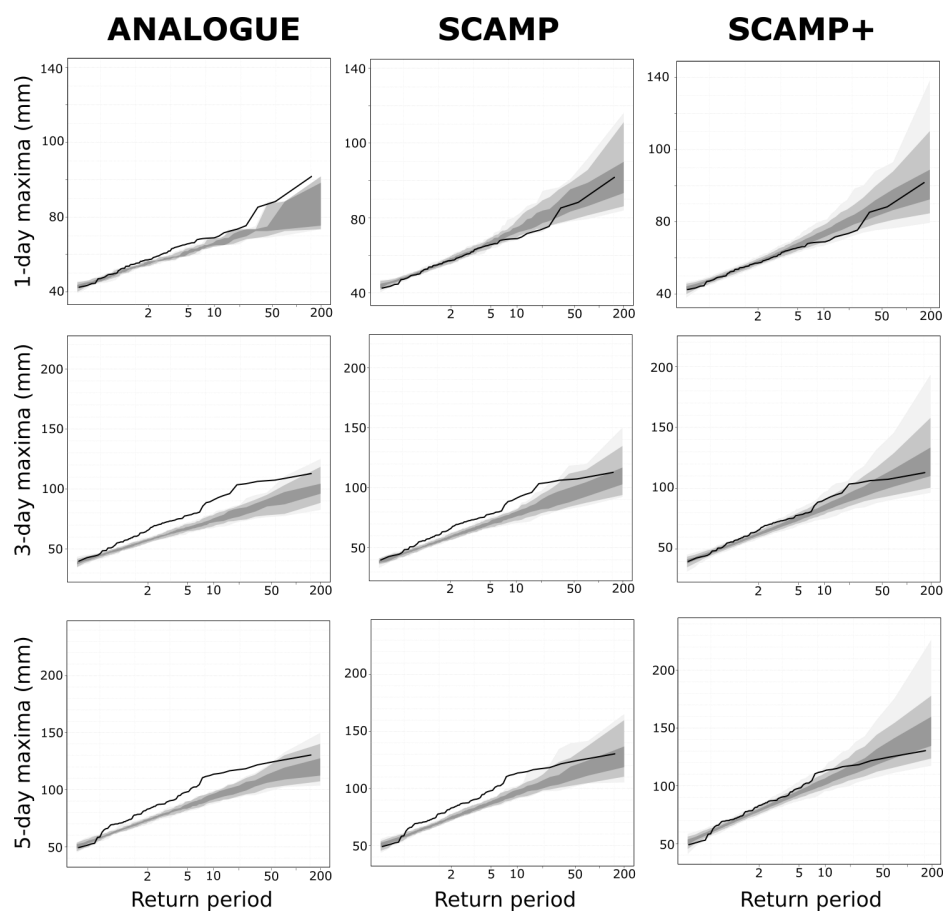
367

368 Considering 1-day extreme events, ANALOGUE is obviously not able to generate precipitation
369 accumulations that exceed the maximum observed one. Combining the analogue method with daily
370 distribution adjustments (SCAMP) overcomes this issue with maximum values reaching 115 mm.
371 SCAMP+ leads to similar results.

372



373 The large underestimation of daily extremes obtained with ANALOGUE leads to an important
374 underestimation of 3-day and 5-day extremes. Despite a better simulation of daily values, SCAMP
375 does not improve significantly the reproduction of 3-day and 5-day extremes. SCAMP+ outperforms
376 both models for all durations, and generates precipitation extremes in agreement with observed
377 extremes. Whatever the return period, the variability between the different 100-year scenarios is
378 larger with SCAMP than with ANALOGUE and much larger with SCAMP+. This again suggests that 3 to
379 5-day extreme events can arise from atypical synoptic conditions, possibly not available in a 110-year
380 long weather archive. Thanks to the random atmospheric trajectories, SCAMP+ is able to generate
381 such conditions.
382



383

384 **Fig.8: Return level analysis of extreme precipitation values associated to model ANALOGUE, SCAMP and**
385 **SCAMP+ for accumulation over 1, 3 and 5 days. The grey shadings present the inter-quantiles intervals (30 x**
386 **111-year scenarios for models ANALOGUE and SCAMP and 300 x 100-year scenarios for SCAMP+).**

387

388



389 5. Discussion

390 The different extensions of the classical analogue method introduced in this study aims at generating
391 long regional weather time series without suffering from the main limitations of analogue models.
392 Indeed, due to the limited extent of the observed time series and the impossibility to simulate
393 unobserved daily scenarios, analogue models usually underestimate observed precipitation
394 extremes. These limitations are relaxed by SCAMP+, the weather generator proposed in this study.
395 SCAMP+ generates unobserved and plausible atmospheric trajectories, and, in addition, provides
396 unobserved samples of temperature and precipitation using daily distribution adjustments. Such a
397 generation process explores a larger weather variability at multiple time scales, which leads to a
398 better reproduction of extremes.

399
400 SCAMP+ is obviously not free of limitations. A first issue is relative to the quality of observations
401 used in the model, especially at the synoptic scale. ERA20C reanalyses used here are produced using
402 sea level pressure and wind measurements only. This guarantees a certain quality of the geopotential
403 at 1000 hPa. The quality of 500 hPa data and of the other predictors is conversely questionable
404 (namely large scale temperature, precipitation and vertical velocities), as they do not benefit
405 from the assimilation of observed data. This may impact the quality of the downscaling method. For
406 instance, this could explain why the mean seasonal cycle of monthly precipitation is not well
407 reproduced in our results (see for instance the underestimation of the mean precipitation in August).
408 Using higher quality data is expected to partly address such limitations. Indeed, using ERA-Interim
409 reanalyses (Dee et al, 2011) instead of ERA20C removes the biases and mis-reproductions mentioned
410 above (not shown), a much larger panel of weather observations being assimilated in ERA-Interim.
411 However, ERA-Interim covers a much smaller time period than ERA20C (roughly 50 years). Using ERA-
412 Interim for our simulations would make the panel of observed synoptic situations much less
413 representative of possible ones, and would impact the ability of our model to generate long-term
414 climate variability. Similarly, the regional predictands time series are based on 105 weather stations
415 for precipitation and 26 weather stations for temperature. The representativeness of this
416 information is also questionable, especially if one is interested in looking at precipitation and
417 temperature extreme events. However, this large number of stations leads to the best possible
418 estimations of these regional variables that can be achieved currently.

419
420 Some other questions remain open, such as the difficulties encountered by SCAMP+ concerning the
421 generation of very hot summers or very cold winters. It is very likely related to the temperature
422 increase experienced over the 20th century, which appears clearly when looking at the hottest
423 summers and the coldest winters. The new weather associations made by the random atmospheric
424 trajectories are mixing days from the 1900s with other from the 2000s, their geopotential analogy
425 being their only selection criteria. This could result in less chance to generate very hot summers (as
426 observed in 2003) or very cold winters (as experienced in 1963). A possible improvement of the
427 method could be to detrend the temperature data and perform the analysis presented in this study
428 on "stationarized" temperature data (similarly to Evin et al., 2018b, see their section 2.2.1).

429
430 All in all, SCAMP+ weather generator paves the way for more developments and applications. As part
431 of the EXAR project (see acknowledgments), the model was coupled with a spatial and temporal
432 disaggregation model and fed a hydrological model in order to generate long series of discharge data



433 (Andres et al., 2019a,b). Additional evaluations on the inter-variable co-variability showed that the
434 physical consistency between temperature and precipitation is well reproduced in our simulations
435 and that the model thus efficiently simulates the precipitation phase and the statistical
436 characteristics of liquid/solid precipitation. SCAMP+ has a low computational cost and is able to
437 generate multiple weather sequences which are consistent with possible trajectories of large scale
438 atmospheric conditions, which motivates future applications to other regions and local weather
439 variables.

440

441 *Data availability.*

442 Precipitation and temperature data have been downloaded from Idaweb
443 (<https://gate.meteoswiss.ch/idaweb/>), a data portal which provides users in the field of teaching and
444 research with direct access to archive data of MeteoSwiss ground-level monitoring networks.
445 However, the acquired data may not be used for commercial purposes (e.g., by passing on the data
446 to third parties, by publishing them on the internet). As a consequence, we cannot offer direct access
447 to the data used in this study. Atmospheric predictors are taken from the European Centre for
448 Medium-Range Weather Forecasts (ECMWF) ERA20C atmospheric reanalysis (Poli et al., 2013),
449 available at the following address: [https://www.ecmwf.int/en/forecasts/datasets/reanalysis-](https://www.ecmwf.int/en/forecasts/datasets/reanalysis-datasets/era-20c)
450 [datasets/era-20c](https://www.ecmwf.int/en/forecasts/datasets/reanalysis-datasets/era-20c).

451

452 *Author contributions.*

453 J. Chardon and D. Raynaud developed the different models considered here. D. Raynaud carried out
454 the simulations, produced the analyses and the figures presented in this study. All authors
455 contributed to the analysis framework and to the redaction.

456

457 *Competing interests.*

458 The authors declare that they have no conflict of interest.

459

460 *Financial support.* We gratefully acknowledge financial support from the Swiss Federal Office for
461 Environment (FOEN), the Swiss Federal Nuclear Safety Inspectorate (ENSI), the Federal Office for Civil
462 Protection (FOCP), and the Federal Office of Meteorology and Climatology, MeteoSwiss, through the
463 project “**Hazard information for extreme flood events on Aare River**” (EXAR):
464 <https://www.wsl.ch/en/projects/exar.html>.

465

466 *Bibliography*

467 Abatzoglou, J. T., & Brown, T. J.: A comparison of statistical downscaling methods suited for wildfire
468 applications. *International Journal of Climatology*, 32(5), 772-780, doi:10.1002/joc.2312, 2012.

469 Ailliot, P., Allard, D., Monbet, V., & Naveau, P.: Stochastic weather generators: an overview of weather
470 type models. *Journal de la Société Française de Statistique*, 156(1), 101-113, 2015.

471 Andres, N., A. Badoux, and C. Hegg.: EXAR – Grundlagen Extremhochwasser Aare-Rhein.
472 Hauptbericht Phase B. Eidg. Forschungsanstalt Für Wald, Schnee Und Landschaft WSL, 2019a.

473 Andres, N., Badoux, A., Steeb, N., Portmann, A., Hegg, C., Dang, V., Whealton, C, Sutter, A., Baer, P.,
474 Schwab, S., Graf, K., Irniger, A., Pfäffli, M., Hunziker, R., Müller, M., Karrer, T., Billeter, P., Sikorska,
475 A., Staudinger, M., Viviroli, D., Seibert, J., Kauzlaric, M., Keller, L., Weingartner, R., Chardon, J.,
476 Raynaud, D., Evin, G., Nicolet, G., Favre, A.C., Hingray, B., Lugrin, T., Asadi, P., Engelke, S.,



- 477 Davison, A., Rajczak, J., Schär, C., Fischer, E.: EXAR – Grundlagen Extremhochwasser Aare-Rhein.
478 Arbeitsbericht Phase B. Detailbericht A. Hydrometeorologische Grundlagen, WSL, Zurich, 2019b.
- 479 Beck, C. H., Jacobeit, J., & Jones, P. D.: Frequency and within-type variations of large-scale
480 circulation types and their effects on low-frequency climate variability in central Europe since
481 1780. *International Journal of Climatology*, 27(4), 473-491, doi:10.1002/joc.1410, 2007.
- 482 Bellier, J., Bontron, G. and Isabella Zin.: Using Meteorological Analogues for Reordering
483 Postprocessed Precipitation Ensembles in Hydrological Forecasting. *Water Resources Research*, 53
484 (12): 10085–107, doi:10.1002/2017WR021245, 2017.
- 485 Boé, J., Terray, L., Habets, F., & Martin, E.: Statistical and dynamical downscaling of the Seine basin
486 climate for hydro-meteorological studies. *International Journal of Climatology: A Journal of the Royal
487 Meteorological Society*, 27(12), 1643-1655, doi:10.1002/joc.1602, 2007.
- 488 Buishand, T. A., & Brandsma, T.: Multisite simulation of daily precipitation and temperature in the
489 Rhine basin by nearest-neighbor resampling. *Water Resources Research*, 37(11), 2761-2776,
490 doi:10.1029/2001WR000291, 2001.
- 491 Caillouet, L., Vidal, J. P., Sauquet, E., & Graff, B.: Probabilistic precipitation and temperature
492 downscaling of the Twentieth Century Reanalysis over France. *Climate of the Past*, 12(3), 635-662,
493 doi:10.5194/cp-12-635-2016, 2016.
- 494 Casanueva, A., Frías, M. D., Herrera, S., San-Martín, D., Zaninovic, K., & Gutiérrez, J. M.: Statistical
495 downscaling of climate impact indices: testing the direct approach. *Climatic change*, 127(3-4), 547-
496 560, doi:10.1007/s10584-014-1270-5, 2014.
- 497 Chardon, J., Favre, A.C., Hingray, B.: Effects of spatial aggregation on the accuracy of statistically
498 downscaled precipitation estimates. *J.HydroMeteorology* 17: 156-1578. doi:10.1175/JHM-D-15-
499 0031.1, 2016.
- 500 Chardon, J., Hingray, B., and Favre, A.-C.: An adaptive two-stage analog/regression model for
501 probabilistic prediction of small-scale precipitation in France, *Hydrol. Earth Syst. Sci.*, 22, 265–286,
502 doi:10.5194/hess-22-265-2018, 2018.
- 503 Chardon, J., Hingray, B., Favre, A. C., Autin, P., Gailhard, J., Zin, I., & Obled, C.: Spatial similarity and
504 transferability of analog dates for precipitation downscaling over France. *Journal of Climate*, 27(13),
505 5056-5074, doi:10.1175/JCLI-D-13-00464.1, 2014.
- 506 Clark, M., Gangopadhyay, S., Hay, L., Rajagopalan, B., & Wilby, R.: The Schaake shuffle: A method
507 for reconstructing space–time variability in forecasted precipitation and temperature fields. *Journal of
508 Hydrometeorology*, 5(1), 243-262, doi:10.1175/1525-7541(2004)005<0243:TSSAMF>2.0.CO;2, 2004.
- 509 Compo, G. P., Whitaker, J. S., Sardeshmukh, P. D., Matsui, N., Allan, R. J., Yin, X., ... & Brönnimann,
510 S.: The twentieth century reanalysis project. *Quarterly Journal of the Royal Meteorological Society*,
511 137(654), 1-28, doi:10.1002/qj.776, 2011.
- 512 Daoud, A. B., Sauquet, E., Bontron, G., Obled, C., & Lang, M.: Daily quantitative precipitation
513 forecasts based on the analogue method: Improvements and application to a French large river basin.
514 *Atmospheric Research*, 169, 147-159, doi:10.1016/j.atmosres.2015.09.015, 2016.
- 515 Dayon, G., Boé, J., & Martin, E.: Transferability in the future climate of a statistical downscaling
516 method for precipitation in France. *Journal of Geophysical Research: Atmospheres*, 120(3), 1023-
517 1043, doi:10.1002/2014JD022236, 2015.



- 518 Dee, D. P., Uppala, S. M., Simmons, A. J., Berrisford, P., Poli, P., Kobayashi, S., ... & Bechtold, P.:
519 The ERA-Interim reanalysis: Configuration and performance of the data assimilation system. *Quarterly*
520 *Journal of the royal meteorological society*, 137(656), 553-597, doi:10.1002/qj.828, 2011.
- 521 Evin, G., Favre, A. C., & Hingray, B.: Stochastic generation of multi-site daily precipitation focusing on
522 extreme events. *Hydrology and Earth System Sciences*, 22(1), 655, doi:10.5194/hess-22-655-2018,
523 2018a.
- 524 Evin, G., Favre, A. C., & Hingray, B.: Stochastic Generators of Multi-Site Daily Temperature:
525 Comparison of Performances in Various Applications. *Theoretical and Applied Climatology*, 1-14,
526 doi:10.1007/s00704-018-2404-x , 2018b.
- 527 Horton, P. & Brönnimann, S.: Impact of Global Atmospheric Reanalyses on Statistical Precipitation
528 Downscaling. *Climate Dynamics* 52 (9): 5189–5211, doi:10.1007/s00382-018-4442-6, 2019.
- 529 Horton, P. Jaboyedoff, M., Metzger, R., Obled, C. and R. Marty: Spatial relationship between the
530 atmospheric circulation and the precipitation measured in the western Swiss Alps by means of the
531 analogue method. *Nat. Hazards Earth Syst. Sci.*, 12, 777–784, 2012.
- 532 Horton, P.; Obled, C.; Jaboyedoff, M.: The Analogue Method for Precipitation Prediction: Finding
533 Better Analogue Situations at a Sub-Daily Time Step. *Hydrol. Earth Syst. Sci.* 21, 3307–3323.
534 doi:10.5194/hess-21-3307-2017, doi:10.5194/nhess-12-777-2012, 2017.
- 535 Kuentz, A., Mathevet, T., Gailhard, J., Hingray, B.: Building long-term and high spatio-temporal
536 resolution precipitation and air temperature reanalyses by mixing local observations and global
537 atmospheric reanalyses: the ANATEM method. *Hydrol. Earth Syst. Sci.*, 19, 2717-2736,
538 doi:10.5194/hess-19-2717-2015, 2015.
- 539 Lafaysse, M., Hingray, B., Mezghani, A., Gailhard, J., & Terray, L.: Internal variability and model
540 uncertainty components in future hydrometeorological projections: The Alpine Durance basin. *Water*
541 *Resources Research*, 50(4), 3317-3341, doi:10.1002/2013WR014897, 2014.
- 542 Lorenz, E. N.: Atmospheric predictability as revealed by naturally occurring analogues. *Journal of the*
543 *Atmospheric sciences*, 26(4), 636-646, doi:10.1175/1520-0469(1969)26<636:APARBN>2.0.CO;2,
544 1969.
- 545 Maraun, D., Wetterhall, F., Ireson, A. M., Chandler, R. E., Kendon, E. J., Widmann, M., ... & Venema,
546 V. K. C.: Precipitation downscaling under climate change: Recent developments to bridge the gap
547 between dynamical models and the end user. *Reviews of Geophysics*, 48(3),
548 doi:10.1029/2009RG000314, 2010.
- 549 Marty, R., Zin, I., & Obled, C.: Sensitivity of hydrological ensemble forecasts to different sources and
550 temporal resolutions of probabilistic quantitative precipitation forecasts: flash flood case studies in the
551 Cévennes-Vivarais region (Southern France). *Hydrological Processes*, 27(1), 33-44,
552 doi:10.1002/hyp.9543, 2013.
- 553 Moberg, A., Jones, P. D., Lister, D., Walther, A., Brunet, M., Jacobeit, J., ... & Chen, D.: Indices for
554 daily temperature and precipitation extremes in Europe analyzed for the period 1901–2000. *Journal of*
555 *Geophysical Research: Atmospheres*, 111(D22), doi:10.1029/2006JD007103, 2006.
- 556 Obled, C., Bontron, G., and Garçon, R.: Quantitative precipitation forecasts: a statistical adaptation of
557 model outputs through an analogues sorting approach, *Atmos. Res.*, 63, 303–324,
558 doi:10.1016/S0169-8095(02)00038-8, 2002.
- 559 Orłowsky, B., & Seneviratne, S. I.: Statistical analyses of land–atmosphere feedbacks and their
560 possible pitfalls. *Journal of Climate*, 23(14), 3918-3932, doi:10.1175/2010JCLI3366.1, 2010.



- 561 Philipp, A., Bartholy, J., Beck, C., Erpicum, M., Esteban, P., Fettweis, X., ... & Krennert, T.:
562 Cost733cat—A database of weather and circulation type classifications. *Physics and Chemistry of the*
563 *Earth, Parts A/B/C*, 35(9-12), 360-373, doi:10.1016/j.pce.2009.12.010, 2010.
- 564 Poli, P., Hersbach, H., Dee, D. P., Berrisford, P., Simmons, A. J., Vitart, F., ... & Trémolet, Y.: ERA-
565 20C: An atmospheric reanalysis of the twentieth century. *Journal of Climate*, 29(11), 4083-4097,
566 doi:10.1175/JCLI-D-15-0556.1, 2016.
- 567 Raynaud, D., Hingray, B., Zin, I., Anquetin, S., Debionne, S., & Vautard, R.: Atmospheric analogues
568 for physically consistent scenarios of surface weather in Europe and Maghreb. *International Journal of*
569 *Climatology*, 37(4), 2160-2176, doi:10.1002/joc.4844, 2017.
- 570 Schefzik, R.: A Similarity-Based Implementation of the Schaake Shuffle. *Monthly Weather Review* 144
571 (5): 1909–21, doi:10.1175/MWR-D-15-0227.1, 2016.
- 572 Srivastav, R. K., & Simonovic, S. P.: Multi-site, multivariate weather generator using maximum entropy
573 bootstrap. *Climate Dynamics*, 44(11-12), 3431-3448, doi:10.1007/s00382-014-2157-x , 2015.
- 574 Steinschneider, S., & Brown, C.: A semiparametric multivariate, multisite weather generator with low-
575 frequency variability for use in climate risk assessments. *Water resources research*, 49(11), 7205-
576 7220, doi:10.1002/wrcr.20528, 2013.
- 577 Stern, R. D., and R. Coe.: A Model Fitting Analysis of Daily Rainfall Data. *Journal of the Royal*
578 *Statistical Society. Series A (General)* 147 (1): 1–34, doi:10.2307/2981736, 1984.
- 579 Surmaini, E., Hadi, T. W., Subagyono, K., & Puspito, N. T.: Prediction of Drought Impact on Rice
580 Paddies in West Java Using Analogue Downscaling Method. *Indonesian Journal of Agricultural*
581 *Science*, 16(1), 21-30, doi:10.21082/ijas.v16n1.2015.p21-30, 2015.
- 582 Van den Besselaar, E. J. M., Klein Tank, A. M. G., & Buishand, T. A.: Trends in European precipitation
583 extremes over 1951–2010. *International Journal of Climatology*, 33(12), 2682-2689,
584 doi:10.1002/joc.3619, 2013.
- 585 Van Den Dool, H. M.: Searching for Analogues, How Long Must We Wait? *Tellus*, 46A (3), 314–324,
586 doi:10.1034/j.1600-0870.1994.t01-2-00006.x, 1994.
- 587 Wilks, D. S., & Wilby, R. L.: The weather generation game: a review of stochastic weather models.
588 *Progress in physical geography*, 23(3), 329-357, doi:10.1177/030913339902300302,1999.
- 589 Yiou, P.: Anawege: a weather generator based on analogues of atmospheric circulation. *Geoscientific*
590 *Model Development*, 7(2), 531-543, doi:10.5194/gmd-7-531-2014, 2014.